LBL-29431
Preprint

Lawrence Berkeley Laboratory
UNIVERSITY OF CALIFORNIA

To be submitted for publication

Scaling and Positive Excess in Secondaries of Nuclear Reactions

T.F. Hoang and H.J. Crawford

August 1990

LOAN COPY
Circulates
for 2 weeks
Bldg. 50 Library.
LBL-29431
Copy 2

Prepared for the U.S. Department of Energy under Contract Number DE-AC03-76SF00098.

DISCLAIMER

This document was prepared as an account of work sponsored by the United States Government. While this document is believed to contain correct information, neither the United States Government nor any agency thereof, nor the Regents of the University of California, nor any of their employees, makes any warranty, express or implied, or assumes any legal responsibility for the accuracy, completeness, or usefulness of any information, apparatus, product, or process disclosed, or represents that its use would not infringe privately owned rights. Reference herein to any specific commercial product, process, or service by its trade name, trademark, manufacturer, or otherwise, does not necessarily constitute or imply its endorsement, recommendation, or favoring by the United States Government or any agency thereof, or the Regents of the University of California. The views and opinions of authors expressed herein do not necessarily state or reflect those of the United States Government or any agency thereof or the Regents of the University of California.

LBL-29431

Scaling and Positive Excess in Secondaries of Nuclear Reactions

T.F. Hoang
1749 Oxford Street
Berkeley, CA 94709

and

H.J. Crawford
Space Science Laboratory
and
Lawrence Berkeley Laboratory
University of California
Berkeley, CA 94720

This work was supported by the Director, Office of Energy Research, Office of High Energy and Nuclear Physics, Nuclear Physics Division, of the U.S. Department of Energy under Contract No. DE-AC03-76SF00098, and by NASA under Grant NGR05-003-513.

Scaling and Positive Excess in Secondaries of Nuclear Reactions*

T.F. Hoang
1749 Oxford Street, Berkeley, CA 94709

and

H.J. Crawford
Space Science Laboratory
and
Lawrence Berkeley Laboratory
University of California
Berkeley, CA 94720

The positive excess of charged particles from p-nucleus reactions is analyzed using the available data from P_{lab} = 20 to 400 GeV/c of CERN and Fermilab experiments. It is found that it originates from a bremsstrahlung type process depending on target $\sim Z^{0.89/3}$ and practically independent of incident energy. At a given energy, the rapidity distributions of $pA \rightarrow h^{\pm} + \cdots$, corrected for the positive excess, determine the same partition temperature as $pp \rightarrow \pi^{-} + \cdots$. This indicates that the primary interaction takes place between the incident proton and one of quasi free nucleon inside the nucleus and leads to a geometrical scaling different from the KNO scaling. A heuristic formula for $\langle n_{ch} \rangle$ is derived on the basis of the properties of secondaries from various p-nucleus reactions.

1. Introduction

One of the remarkable features of particle production by p-nucleus reactions is that the multiplicity of shower particles turns out to be very much like that of pp collisions at the same energy, reflecting the space-time evolution of high-energy hadronic collisions.[1] As a consequence, the nuclear effect appears to play a lesser role in the investigation of multiparticle production by nuclear reactions, in spite of the fact that the difference between the positive and the negative secondaries is not small at all, and that the positive excess may affect critically certain parameterizations such as the partition temperature T_p of the Chou-Yang-Yen (CYY) model.[2]

From the point of view of physics, it is imperative to know the nature of these positive particles in excess over the negative ones. How do they differ from the negatives which are produced by the soft process? Another important problem is the scaling. As is well known, scaling is an important property for non-diffractive particle production by pp collisions. The question arises: How does scaling behave in the case of p-nucleus reactions?

The purpose of the present work is to investigate these outstanding problems using currently available high-energy p-nucleus data. We will study the behavior of the positive excess in terms of the rapidity distributions using a CERN-SPS experiment by the NA5 Collaboration[3] and a recent Fermilab experiment E565-570[12], both at P_{lab} = 200 GeV/c (Sec. 2), and its effect on the estimates of T_p^* according to the CYY formula (Sec. 3). We find T_p^* about twice that of the negatives of the same experiment. Then we consider an appropriate formula to correct the charged y distributions of the positive excess so that T_p^* thus estimated is equal to that of the negative secondaries (Sec. 4). We find that the correction term is practically independent of energy, whereas its A dependence has a simple property of geometric aspect. Our analysis of the positive excess indicates that it is produced by a process like the bremsstrahlung[4] in contrast with the production of negative secondaries (Sec. 5). We will see that our correction method applies also to a p-emulsion experiment at 200 GeV/c [14] (Sec. 7).

We will see that the y distributions of shower particles from pA reactions at the same energy, after correction for the positive excess, lead practically to the same T_p^*, indicating a geometrical scaling in the sense of the CYY model (Sec. 6) as has been reported in a previous work for the negative secondaries.[5] On the other hand, we find that the well established KNO scaling holds only in the projectile region of p-nucleus reactions at different energies. A semi-empirical formula for the multiplicity of shower particles will be given on general grounds of the geometrical aspect of p-nucleus reactions.

2. Characteristics of secondaries of $p + A \rightarrow h^{\pm} + \cdots$

Consider, to fix our ideas, the CERN-SPS experiment of pA reactions at $P_{lab} = 200$ GeV/c by the NA5 Collaboration.[3] They have measured in the lab system the rapidity $y = \frac{1}{2} \ln [(E+P_{\parallel})/(E-P_{\parallel})]$ distributions of positive, negative and "all" particles for p, Ar and Xe targets. A detailed analysis of y distributions of their $p + A \rightarrow \pi^- + \cdots$ data has already been reported elsewhere.[5] Let us compare, to begin with, the positive and the negative y-distributions of pp as is shown in Fig. 1, error bars being omitted for simplicity.

Clearly, we see that the y distribution of π^+ is much broader than that of π^-. This difference indicates that, besides the soft process which produces the negative pions, there exists another process contributing to the excess of π^+ compared to π^-. We are going to investigate this process in the following sections.

Let us first analyze these two rapidity distributions in terms of the partition temperature model of Chou, Yang and Yen[2] as in our previous work.[5] We use the generalized CYY formula in the cms of the incident proton and a quasi-free nucleon of the target nucleus, namely

$$\frac{1}{N}\frac{dn}{dy} = \frac{C}{\left(\alpha + \frac{1}{T_p^*}\cosh(y-y^*)\right)^2} \tag{1}$$

where C is the normalization coefficient, α a fixed parameter

$$\alpha = 2 / \langle P_{\perp} \rangle \tag{2}$$

and the two free parameters are: the shift parameter y* with respect to the cms and the partition temperature T_p^* in the fineball (FB) system specified by the asterisk. The kinematic properties of the FB being discussed elsewhere,[5] suffice it to recall, in passing, that the Lorentz transformation of y amounts to a translation, e.g., the passage of the cms to the lab system where the NA5 data are measured is $y' = y + y_{cm}$ with

$$y_{cm} = \frac{1}{2} \ln \left(\frac{2P_{lab}}{m_p} \right) = 3.03 \tag{3}$$

the cms rapidity with respect to the lab system.

We have performed fits to the y distributions in Fig. 1 by means of (1), with $\alpha = 5.46$ according to (2), for $|y| \leq y_{cm}$. The fits as shown in Fig. 1 are satisfactory. The parameters are listed in Table I. Note in particular that the partition temperature T_p^* of π^+ is much larger than that of π^-, by a factor ~2.5. The same situation has been found for pAr and pXe reactions, see Table I, indicating a large overestimation of T_p^* without correcting the positive excess.

In this regard, it should be mentioned that according to the CYY formula (1), the shape of the rapidity distribution depends essentially on αT_p^* and that the estimate of αT_p^* is determined by the inflection point of the distribution corresponding to y_0 given by

$$2 \cosh^2 (y_0 - y^*) - \alpha T_p^* \cosh (y_0 - y^*) - 3 = 0 \,. \tag{4}$$

It is easily seen from (4) that a larger αT_p^* of the y distribution of π^+ corresponds to a farther inflection point compared to that of π^-, because of the background due to the excess of π^+.

3. The positive excess of inclusive $p + A \rightarrow \pi^+ + \cdots$.

Next we investigate the behavior of the background in the y distributions of positive secondaries compared to the negative ones. For this purpose, we consider, for each pA reaction

$$\Delta(A) = \left(\frac{1}{N} \frac{dn}{dy} \right)_+ - \left(\frac{1}{N} \frac{dn}{dy} \right)_- \tag{5}$$

using the data of the NA5 experiment.[5] The result is summarized in Fig. 2.

Consider first the pp case, we note that the statistical fluctuations of the plot are rather large. As $pp \rightarrow \pi^+ + \cdots$ is symmetric in view of the parity conservation, we may fold the plot around the cms axis to reduce the fluctuations. The folded plot shown in Fig. 3(a) seems to increase with $|y|$ as is indicated by the dotted line of the least-squares fit, namely,
$\Delta(1) = (0.192 \pm 0.015) + (0.039 \pm 0.056)\,|y|$. As the slope is consistent with zero, $\Delta(1)$ is actually independent of y, its average being $\bar{\Delta} = 0.24 \pm 0.10$.

That $\Delta(A)$ is constant is further corroborated by the result of another experiment at $P_{lab} = 205$ GeV/c by ANL[6] as shown in Fig. 3(b). Here, we find a different pattern, rather of random nature; the average $\bar{\Delta} = 0.27 \pm 0.09$ is comparable to the NA5 data.

Furthermore, we note that this average 0.24 for pp is consistent with those of pAr and pXe in the forward direction corresponding to the fragmentation of the proton projectile, see Table I, as is expected from the property of limiting fragmentation observed in the p-nucleus reactions.

We are therefore led to assume that in a definite region of the y distribution, forward (FD) or backward (BD) in the cms of p-nucleon collision, the difference $\Delta(A)$ defined by (5) follows a random distribution along the y axis; in other words, independent of y.

The FD and BD averages of $\Delta(A)$ for the NA5 experiments we are dealing with are shown by the horizontal straight lines in Fig. 2; their values are listed in Table 1. Note that the gap between the BD and the FD averages increases with the target size. We will discuss this point in Sec. 5.

4. Positive excess correction

The knowledge of the FD ($y > 0$) averages of the positive excess enables us to estimate T_p^* using the corrected y distributions of <u>charged</u> particles (albeit shower particles). From our definition of Δ, Eq. (5), we may write

$$\left(\frac{1}{N}\frac{dn}{dy}\right)_{corr} = \frac{1}{2}\left[\left(\frac{1}{N}\frac{dn}{dy}\right)_{ch} - \Delta(A,y)\right] \tag{6}$$

the values of the correction term Δ being listed in Table I for the NA5 experiments.

As a validity test of our simple substraction method, Eq. (6), we have carried out fits to the charged y distribution of the pp case of the NA5 data[3] with the CYY formula (1) applied to the corrected y distribution according to (6), assuming successive values of $\Delta(1) = 0$, to 0.4. We find a broad minimum of χ^2/point at $\Delta \simeq 0.25$, in agreement with the average $\bar{\Delta} = 0.24$ listed in Table I.

Thus we proceed to fit the charged y distributions of the NA5 experiments[3] twice. First, we fit the raw data assuming $\alpha = 5.46$ and $|y| \leq y_{cm}$ as before, without correction (shown by the dotted lines). Next we refit the corrected data according to (6) and using the same condition (shown by solid lines). The fits for pp and pXe are shown in Fig. 4, the pAr case being omitted for simplicity. The parameters of fits are listed in Table I.

For comparison, we have plotted in the same figure the y distributions of negatives. Note that the difference between charged and negative secondaries is less conspicuous than in the case of positive and negative ones shown in Fig. 1.

If we compare the estimates of T_p^* for charged secondaries in Table I, with and without correction, we note that the values of T_p^*, without correction, are always larger than those with correction, about by a factor ≥ 2.

Finally, it is interesting to note that for the nuclear targets, just as in the previous case of $pp \rightarrow h^{\pm} + \cdots$ (charged secondaries), we find about the same T_p^* with the corrected y distributions of charged secondaries as in the case of negative secondaries. This consistency test justifies the subtraction method we have used to correct the positive excess.

5. Properties of $\Delta(A)$

If we represent the values of $\Delta(A)$, Eq. (5), for inclusive $p + A \rightarrow h^{\pm} + \cdots$ of the NA5 experiment,[3] listed in Table I, in a semi-log plot vs. Z of the target, as shown in Fig. 5, we find an almost linear dependence leading to

$$\Delta(A) = c \; Z^{\alpha/3} \; . \tag{7}$$

We find by the least-squares fit

$$c = 0.24 \pm 0.02, \qquad \alpha = 0.89 \pm 0.11 \quad .$$

The fit shown by the dashed line is satisfactory.[7]

It is interesting to note that

$$c \simeq \Delta(1), \tag{8}$$

namely, the fit passes through the point for the proton target, whereas $\alpha \simeq 1$ reflecting the geometric property of the mechanism giving rise to the excess of the produced π^+ compared to π^-.

In view of (8), we may write the A-dependence of the correction term in (6) as follows, using the Heaviside function:

$$\Delta(A,y) = \Delta(1)Z^{[1-H(y)]\alpha/3} \quad . \tag{9}$$

It follows that for its energy dependence, we need only to investigate the case of $p + p \rightarrow h^{\pm} + \cdots$. We have analyzed the data of other experiments.[8] In Fig. 6, we plot the values of $\Delta(1)$ against P_{lab} from 12 to 400 GeV/c.

We note that the energy dependence of $\Delta(1)$ is rather weak. Now, according to the results of the Rochester experiments,[8(b)] the heights of the y distributions for π^+ and π^- secondaries of pp collision rise rather slowly with the energy as expected from the Muller approach.[9] Consequently, we may assume

$$\Delta(1) = a - \frac{b}{s^{1/4}} \tag{10}$$

and find by the least-squares fit

$$a = 0.248 \pm 0.013, \qquad b = 0.092 \pm 0.056 \quad .$$

The fit is shown by the solid curve in Fig. 6. Here again, we find b consistent with zero, indicating that to a good approximation we may neglect the energy dependence of the correction term in Eq. (5).

6. Scaling property of $p + A \rightarrow h^{\pm} + \cdots$ at the same energy.

In a previous work,[5] a scaling property has been observed for charged secondaries of heavy-ion reactions at 200 GeV/nucleon of a CERN-SPS experiment WA80,[11] no correction being made of the excess of positive secondaries. We have to examine more carefully this important property using y distributions of a recent Fermilab experiment, E565/570, of p-nucleus reactions at $P_{lab} = 200$ GeV/c.[12]

Their data for shower particles from p, Mg, Ag and Au targets are reproduced in Fig. 7. The curves represent the fits using the CYY formula (1) with $\alpha = 5.46$ and $|y| \leq 3.03$ as in the case of the NA5 experiment. The parameters y^* and T_p^* are listed in Table II, typical errors being $\Delta y^* \simeq 0.04$ and $\Delta T_p^*/T_p^* \simeq 14\%$. Note that except for the Mg target, here also, we find $T_p^* \gtrsim 1$ GeV as in the case of the NA5 experiment (Table I) and that $y^* \neq 0$ for pp is probably systematic, since it should be zero within statistical errors as is required by the parity conservation of the pp system.

Next, let us consider the corrected y distributions by subtracting in each case an appropriate corrected term $\Delta(A)$ according to (7). The results are shown in Fig. 8. The curves represent new fits with the CYY formula (1), and the parameters are listed in Table II. It is interesting to note that here again we find T_p^* about equal to one half that of the uncorrected y distributions, just as in the case of the NA5 data (Sec. 4), and that they are now comparable to the T_p^* of $p + p \rightarrow \pi^- + \cdots$ at the same energy of the NA5 experiment. This justifies the substraction method and the empirical formula Eq. (7) for $\Delta(A)$.

We now discuss the scaling of inclusive $p + A \rightarrow h^{\pm} + \cdots$ reactions <u>at the same energy</u>, in the context of the partition temperature model of Chou, Yang, and Yen.[2] In this regard, we recall that there are two free parameters in (1), the shift parameter y^* and the partition temperature T_p^*, whereas the normalization coefficient C is related to the average multiplicity, which, in turn, is $\sim A^{1/3}$ as has been reported in our previous work.[3] As for a given energy, $\langle P_{\perp} \rangle$ is practically independent of the nature of the target, the same is found for T_p^* of corrected y distributions, we therefore expect scaling to hold in the FB system corresponding to zero of the shift parameter.

Therefore, for each target A, we consider a scaled y distribution:

$$\rho(A,y) = \frac{1}{A^{1/3}}\left[\left(\frac{dn}{dy}\right)_{ch} - \Delta(A,y)\right] \tag{11}$$

and plot it against $y - y^*$ to go to the FB system. The results are shown in Fig. 9. We note that scaling holds especially well in the central region for all three targets: Mg, Ag and Au, whereas the Mg target deviates somehow from the other two in the region of target fragmentation, suggesting that scaling may hold better for large targets.

With this in mind, we perform an overall fit to the three scaled distributions for $|y-y^*| \leq 2$ instead of 3 in order to leave aside the deviated points outside the central region. We find

$$T_p^* = 0.669 \pm 0.050 \text{ GeV}$$

$$y^* = 0.34 \pm 0.05$$

The fit is shown by the solid curve in Fig. 9(a), its extrapolations being indicated by the dashed lines. We find the fit satisfactory and T_p^* in agreement with that of $p + p \rightarrow \pi^- \cdots$ (Table I), except that the new shift parameter differs from zero as can be seen from the plot in Fig. 8. This lack of symmetry may be due some unknown systematics.

Finally, we note that the trend of scaling remains even without correction due to the positive excess as i seen from Fig. 9(b) and that a similar fit using the CYY formula (1) for $|y-y^*| \leq 2$ as before seems also satisfactory. Nonetheless, the parameters are quite different:

$$T_p^* = 1.045 \pm 0.165$$

$$y^* = -0.14 \pm 0.04$$

We now find T_p^* comparable to those of <u>charged</u> secondaries of pA, about twice those of negative ones as is listed in Table II. It is this scaling that has been observed with the heavy-ion reactions reported in the previous work.[5]

7. Inclusive p + Em reaction.

Besides the rapidity distributions we have analyzed in the previous sections, there exist a great wealth of pseudorapidity distributions, $\eta = \ln(\cot \theta/2)$, at all energies, especially from the accumulated work of photoemulsion technique.

Obviously, at high energy, m_π is negligible, so $\eta = y$. However, as is well known, the two distributions, rapidity on the one hand and pseudorapidity on the other, have different shapes in the central region, beyond that they are practically the same, especially in the fragmentation regions.[13] As the estimation of T_p^* depends essentially on the part of the η distribution near the average $\langle|\eta|\rangle$[14] we may treat the η distribution on an equal footing with the y distribution.

As regards the complexity of the inclusive $p + Em \rightarrow h^\pm + \cdots$ data caused by the chemical compounds constituent of the emulsion, there is always this important question: How to extract any reliable information on the primary interaction, namely, the collision of the incident proton with one nucleon of various nuclei contained in the emulsion?

For this purpose, we have considered a fictitious compound target like BrAg in emulsion, composed of MgAg instead and computed the expected η distribution using the data of pMg and pAg data analyzed in the previous section and combining them by weighting over their cross-sections, i.e., $\sim A^{2/3}$ for simplicity. Then we fit the simulated η distribution with the CYY formula (1). We get $\eta^* = -0.04$ and $T_p^* = 0.880 \pm 0.063$ comparable to the averages (arithmatic) of y^* and T_p^* for Mg and Ag in Table II.

We therefore proceed to analyze the p + Em data for BrAg at $P_{lab} = 200$ GeV/c by Hebert et al.[15] using the CYY formula (1). Their data are shown in Fig. 10(a), the fit is satisfactory. We get

$$\eta^* = -0.55 \pm 0.05 \quad , \quad T_p^* = 1.040 \pm 0.143 \text{ GeV}$$

comparable to the Ag target listed in Table II.

As regards the correction according to (6), we use the effective Z weighted over $A^{2/3}$ of Br and Ag: $Z_{eff} = 41.5$ to compute $\Delta(A)$ by (7). The corrected η distribution is shown in Fig. 10(b), the solid curve being the fit with (1). The parameters are:

$$\eta^* = -0.39 \pm 0.08 \quad , \quad T_p^* = 0.603 \pm 0.093 \text{ GeV} \quad .$$

It is worth noting that we get T_p^* consistent with that of $p + p \rightarrow \pi^- + \cdots$ at the same energy (see Table I) within one standard error. This justifies a posteriori the validity of the method and the empirical formula Eq. (7) we have used to correct the data.

8. Energy dependence and KNO scaling

We have observed the scaling of corrected y distributions of *shower* particles from various p-nucleus reactions at the same energy (Sec. 6). We now investigate another scaling, the well established KNO scaling for hadronic collisions.[16] For this purpose, we have analyzed other available p-nucleus data at different energies to compare with the 200 GeV/c data discussed in the previous sections.

For brevity, we content ourselves with the data of p + Cu at $P_{lab} = 50$ GeV/c by the Max Planck Institute (MPL)[17] and p + Al at 360 GeV/c by the EHS-RCBC Collaboration,[18] other data being similar with larger experimental uncertainties. The pseudorapidity (in cms) distributions are shown in Fig. 11(a), the typical errors ~2.5% for the MPI data and ~3% for the other being omitted for simplicity. The curves are fit with the CYY formula (1) for $|\eta| \leq \eta_{cm}$, the parameters are listed in Table III together with some characteristics of their experiments.

We note that the fits are very satisfactory and that the two distributions are quite different as can be seen from their widths, so are their T_p^* values. This rules out the geometrical scaling based on the CYY model discussed in Sec. 6.

Next, we make corrections for these distributions using the method outlined in Sec. 4. The results are shown in Fig. 11(b) together with the new fits using (1), assuming the same $\alpha = 5.46$ as in the previous fits with correction. The parameters are summarized in Table III. The fits are

satisfactory. Note that here as in the previous cases of 200 GeV/c data, the values of T_p^* are about equal to one half those without correction.

We now investigate the KNO scaling using these distributions (we assume $y = \eta$) and those of 200 GeV/c. We plot the corrected η distribution of shower particles scaled by the average multiplicity $\langle n_{ch} \rangle$ against the shifted η scaled by the average $\langle |\eta| \rangle$, namely vs. $(\eta - \eta^*)/\langle |\eta| \rangle$. The results are shown in Fig. 12.

An inspection of this plot reveals that in the forward direction of the incident proton the KNO scaling holds as in expected from the well-known limiting fragmentation. We note this kind of scaling in terms of the reduced pseudorapidity $\eta/\langle |\eta| \rangle$ has been observed for pp by Nakamura and Kudo.[19] However, in the backward direction corresponding to the target fragmentation, the behavior is quite different. Indeed, if we compare this KNO scaling plot with Fig. 9 showing the geometrical scaling of $p + A \rightarrow h^{\pm} + \ldots$ at the same energy $P_{lab} = 200$ GeV/c, we note a significant difference, suggesting that the KNO scaling is not universal, namely, it holds only for the fragmentation of the projectile proton but not for the fragmentation of the target nucleus in general. Our conclusion agrees to some extent, with the result of the Fermilab experiment,[12] their analysis being based on the statistical grounds, namely, the behavior of the dispersion of the multiplicity distribution.

9. The charged multiplicity

In a previous work to investigate the properties of inclusive $p + A \rightarrow \pi^- + \cdots$, we have found that the negative multiplicity may be expressed in terms of $p + p \rightarrow \pi^- + \cdots$ at the same energy as follows:[5]

$$\langle n_- \rangle_{pA} = \frac{1}{2} \langle n_- \rangle_{pp} \, (1 + A^{\alpha'/3}) \tag{12}$$

with

$$\alpha' = 0.80 \pm 0.16 \, ,$$

As we now know the behavior of the excess $\varepsilon(A)$ of positive secondary over negative ones, namely, according to (7)

$$\varepsilon(A)/Y = \Delta(1) + \Delta(1)\bullet Z^{\alpha/3} \tag{13}$$

where Y is the rapidity interval

$$Y = 2y_{cm} \simeq \ln \frac{s}{m_p^2} \tag{14}$$

It is straightforward to write a closed form for the charged multiplicity of p-nucleus reactions.

In this regard, we recall that the factor $\langle n_- \rangle_{pp}$ in (12) serves merely to express the energy dependence of the multiplicity of pA and that in the context of the fireball (FB) model, the negative multiplicity of pp may be written as[20]

$$\langle n_- \rangle_{pp} = 2\alpha_p(\gamma_{c.m}/\gamma_{FB} - 1) \tag{15}$$

where γ_{FB} is the Lorentz factor of the FB with respect to the cms and $\alpha_p = 0.26$ is a parameter, the subscript p is used to distinguish pp from other reactions as is discussed in Ref. 20. By FB we mean the rest-frame of secondaries in one hemisphere of the cms of pp. We recall that owing to the scaling,

$$\gamma_{c.m}/\gamma_{FB} = 2\sqrt{\gamma_{c.m.} - 1} - 1 \quad . \tag{16}$$

With these remarks, we may write explicitly the following expression for the charged multiplicity of p-nucleus reactions

$$\langle n_{ch} \rangle_{pA} = N(2\sqrt{\gamma_{c.m.} - 1} - 1)\ (1 + A^{\alpha'/3}) + \Delta(1)(1 + Z^{\alpha/3})\ Y \tag{17}$$

where $\alpha = 0.80$ (see Eq. (12)), $\alpha' = 0.89$ (see Eq. (7)), $\Delta(1) = 0.24$ (see Eq. (11) and N is a coefficient to be determined by fitting the experimental values of charged multiplicity analyzed in the present work, except the case of pEm.[21] We find

$$N = 0.36 \pm 0.03 \quad .$$

In Fig. 13 we have plotted the experimental values of charged multiplicity vs. the values predicted by (17). That all the points are situated close to the bisector (solid line) indicating the correctness of our formula and consequently justifies the validity of our method of analysis.

As a further check, we have considered another case outside the fitting range corresponding to $P_{lab} \leq 50$ GeV, namely, p + Ne at 28 GeV/c by Miller and Nowak.[22] Their datum and the computed $\langle n_{ch} \rangle$ (17) are shown by the triangle in Fig. 13. Here also, we find it very close to the bisector.

10. Remarks

We have investigated the positive excess of secondaries from p-nucleus reactions. We find that these particles, presumably π^+ mesons, have a random distribution along the rapidity axis indicating that they are emitted by a bremsstrahlung-type mechanism, in contrast to the soft process emitting the π^- mesons. The A dependence of this positive excess is approximately geometric, e.g., $\sim Z^{\alpha/3}$ with $\alpha = 0.89$, just like that of the negative multiplicity.[5]

A simple subtraction method is derived to correct the effect of the positive excess on the estimation of the partition temperature T_p^* determined by the generalized CYY formula (1). We find the overestimation of T_p^* without correction rather important, by a factor of ~2 compared to T_p^* of negative secondaries. The T_p^*'s from the corrected y distributions are about the same as that of negatives, which in turn is equal to $p + p \rightarrow \pi^- + \cdots$ at the same energy. This indicates that, in the multiparticle production by p-nucleus reaction, the primary interaction takes place between the incident proton and a quasi free nucleon inside the target nucleus.

We find a new geometric scaling for inclusive $p + A \rightarrow h^{\pm} + \cdots$ reactions at the same energy. It is based on this remarkable property that such reactions have approximately the same T_p^*, irrespective of the nature of the target. This scaling is essentially different from the KNO scaling which is found to hold only for the fragmentation of the incident proton, but not for the fragmentation of the nuclear target, reflecting the complexity of nuclear production of particles compared to pp collisions.

Acknowledgements

The authors benefitted from many discussions and comments with I. Hinchliffe and G. Gidal and thank them for their constant interest in the work. One of the authors (TFH) would like to thank L. Wagner for encouragement, Space Science Laboratory and Tsi Jung Fund for support.

References and Footnotes

1. K. Gottfried, in High Energy Physics and Nuclear Structure, Proc. of the Vth Int. conf., Uppsala, 1973, Ed. G. Tibell (North Holland, Amsterdam, 1974), p. 79 and Phys. Rev. Lett., 32, 957 (1974).
2. T.T. Chou, Chen Ning Yang and E. Yen, Phys. Rev. Lett., 54, 510 (1985).
3. NA5 Collaboration, C. de Marzo, et al., Phys. Rev. D 26, 1019 (1982) and 29, 2476 (1984).
4. R. Feynman, in High Energy Collisions, Ed. C. N. Yang, et al. (Gordon and Breach, New York, 1969), p. 237.
5. T.F. Hoang and H.J. Crawford, Phys. Rev. D 42, 45 (1990).
6. ANL experiment, T. Kofka, et al., Phys. Rev. D 16, 1261 (1977).
7. We have also tried another form: $\Delta(A) = c'A^{\alpha'/3}$ and got $c' = 0.24 \pm 0.2$ and $\alpha' = 0.66 \pm 0.04$. but the fit is much worse, with a $\chi^2 = 0.52$ instead of 0.35 in the case of (7).
8. We have used the data of the following experiments: (a) $P_{lab} = 12$ and 24 GeV/c, V. Blodel, et al., Nucl. Phys. B 69, 454 (1974) and $P_{lab} = 102$ and 400 GeV/c, C. Bromberg, et al., Nucl. Phys. B 107, 82 (1976).
9. A. Muller, Phys. Rev. D 2, 2963 (1970).
10. We used the $pp \rightarrow \pi^- + \cdots$ data analyzed in a previous work: T.F. Hoang and H.J. Crawford, Z. Phys. C 43, 215 (1989).
11. WA80 Collaboration, A. Albrecht, et al., Phys. Lett. 202, 596 (1988).
12. Fermilab experiment E565/570, D.H. Brick, et al., (a) Phys. Rev. D 39, 2484 (1989) and (b) ibid., 41, 765 (1990).
13. See e.g., the UA5 Collaboration, G.J. Alner, et al., Nucl. Phys. B 291, 445 (1987).
14. T.F. Hoang, Zeit. für Phys. C 45, 321 (1989).
15. G. Hebert, et al., Phys. Lett., 48B, 467 (1974) and Phys. Rev. D 15, 1867 (1977). We have used the data compiled for pE_m by S. Frederickson, et al., Phys. Rep. 144C, 187 (1987).
16. Z. Koba, H.B. Nielsen and P. Olesen, Nucl. Phys. B40, 317 (1972).

17. Max Planck Institute Experiment, K. Braune, et al., Zeit. für Phys. C 17, 105 (1983).

18. EHS-RCBC Collaboration, J.L. Bailly, et al., Zeit. für Phys. C 35, 301 (1987).

19. E.R. Nakamura and K. Kudo, Zeit für Phys. C 40, 81 (1989).

20. T.F. Hoang, (a) Phys. Rev. D 12, 296 (1975) and (b) ibid., 24, 1406 (1981).

21. Assuming $A_{eff} = 93.5$ and $Z_{eff} = 41.5$, averages over $A^{2/3}$ of Br and Ag, we get by (17); $\langle n_{ch} \rangle = 17.6$ compared to 14.7 ± 0.5 reported by the authors of the experiment Ref. 14.

22. D.J. Miller and R. Nowak, Nuovo Cimento Lett. 13, 39 (1975).

Table 1. Characteristics and parameters of rapidity distributions of $p + A \rightarrow h^{\pm} + \cdots$ 200 GeV/c = NA22 experiment, Ref. 5. N.B. y* is referred to the c.m.s.

		pp	pAr	pXe
$\langle P_{\perp} \rangle$ (MeV/c)		366 ± 2	376 ± 1	363 ± 3
$\langle n \rangle_{all}$		7.27 ± 0.06	14.98 ± 0.45	20.67 ± 2.40
Δ(A)	BD y < 0	0.23 ± 0.07	0.44 ± 0.15	0.83 ± 0.16
	FD y > 0	0.24 ± 0.12	0.30 ± 0.09	0.29 ± 0.04
y distribution				
negat.	y*	0	–0.46 ± 0.03	–0.66 ± 0.01
	T_p^* (GeV)	0.547 ± 0.049	0.816 ± 0.737	0.642 ± 0.062
posit.	y*	0.12 ± 0.05	–0.68 ± 0.03	–1.26 ± 0.08
	T_p^* (GeV)	1.430 ± 0.05	1.854 ± 0.302	2.550 ± 0.369
all	y*	0.06 ± 0.05	–0.55 ± 0.05	–0.96 ± 0.06
	T_p^* (GeV)	1.013 ± 0.125	1.258 ± 0.205	1.615 ± 0.157
Corrected Δ(A)				
all	y*	0.15 ± 0.07	–0.60 ± 0.05	–1.04 ± 0.07
	T_p^* (GeV)	0.514 ± 0.047	0.644 ± 0.105	0.680 ± 0.073

Table II. Parameters of rapidity distributions of shower particles of inclusive p + A reactions at 200 GeV/c, Fermilab E 565/570, Ref. 12. Typical errors $\Delta y^* = \simeq 0.05$ and $\Delta T_p^*/T_p^* \simeq 14\%$. N.B. $\alpha = 2/\langle P_\perp \rangle = 5.46$ and y* is referred to the c.m.s.

	pp	pMg	pAg	pAu
$\langle n_{ch} \rangle$		13.1 ± 0.9	18.1 ± 0.7	21.6 ± 1.2
y*	0.12	–0.24	–0.77	–1.04
T_p^* (GeV)	1.210	0.627	1.203	1.177
With correct.				
y*	0.17	–0.08	–0.55	–0.92
T_p^* (GeV)	0.663	0.320	0.724	0.590

Table III. Characteristics and parameters of p + A reactions, Refs. 14 and 15. Fit errors $\Delta\eta^* \simeq 0.04$ and $\Delta T_p^*/T_p^* \simeq 14\%$. N.B. η^* is with respect to the cms.

	pCu	pAl
P_{lab} (GeV/c)	50	360
$\langle n_s \rangle$	10.30 ± 0.26	17.7 ± 1.5
$\langle P_\perp \rangle$ (GeV/c)	0.332	0.372
η_{cm}	2.67	3.32
η^*	–0.57	–0.72
T_p^*	0.547	2.028
with correct.		
η^*	–0.52	–0.59
T_p^*	0.234	1.286
$\langle \lvert\eta\rvert \rangle$	1.02	1.26

Figure Captions

Fig. 1. Rapidity distributions in the lab system of π^+ and π^- from inclusive pp at $P_{lab} = 200$ GeV/c by NA5 collaboration, Ref. 3. The curves represent the fits with the CYY formula (1), the parameters are in Table I.

Fig. 2. Plots of the positive excess of secondaries vs. y' (rapidity in the lab system) for inclusive pp, pAr and pXe at 200 GeV/c, NA5 data, Ref. 3. The dash straight lines represent the averages in the projectile and the target region.

Fig. 3. Folded plots of positive excess $\Delta(1)$ of inclusive pp at ~200 GeV/c. (a) NA5 data, Ref. 3 and (b) ANL data, Ref. 6. The variations of $\Delta(1)$ are shown by the dotted lines, see text.

Fig. 4. Rapidity distributions of charged (crosses) and negative (circles) secondaries of pp and pXe at 200 GeV/c, NA5 data, Ref. 3. The solid lines are CYY fits without correction; the dotted lines are fits with correction according to Eq. (6). The parameters are in Table I.

Fig. 5. The Z dependence of the positive excess $\Delta(A)$ for $pA \rightarrow h^{\pm} + \cdots$ at 200 GeV/c of NA5 experiment, Ref. 3. The dotted line represents the fit: $\Delta(A) = cZ^{\alpha/3}$ with $c = 0.24 \pm 0.02$ and $\alpha = 0.89 \pm 0.11$.

Fig. 6. Energy dependence of the positive excess $\Delta(1)$ for inclusive $pp \rightarrow \pi^{\pm} + \cdots$ the curve is a fit according to the Muller approach, see text.

Fig. 7. Rapidity distributions of $p + A \rightarrow h^{\pm} + \cdots$ at $P_{lab} = 200$ GeV/c, Fermilab experiment E 562/570, Ref. 12. The curves represent fits with Eq. (1). The parameters are in Table II.

Fig. 8. Charged rapidity distributions of $p + A \rightarrow h^{\pm} + \cdots$ at $P_{lab} = 200$ GeV/c with correction for the positive excess. Fermilab experiment E 562/570, Ref. 12. The parameters are in Table II.

Fig. 9. Replot of Fermilab data in Figs. 7 and 8 with $\frac{1}{N}\frac{dn}{dy}$ scaled by $A^{1/3}$ against y (in cms) and shifted by y* of the fits with CYY formula (values of y* in Table II). (a) without correction and (b) with correction for the positive excess. The solid curves represent overall fits using Eq. (1), the dotted lines being extrapolations; scaling requires the superpositions of the scaled distributions.

Fig. 10. Pseudorapidity distributions of p-emulsion experiment at 200 GeV/c by Hebert, et al., Ref. 15, with and without the correction for the positive excess assuming $Z_{eff} = 41.5$.

Fig. 11. Rapidity distributions of p + Cu and p + Al at 50 and 360 GeV/c, respectively, data of MPI, Ref. 17 and EHS-RCBC, Ref. 18. (a) Without correction and (b) with correction for the positive excess. the curves represent fits with Eq. (1). The parameters are in Table III.

Fig. 12. The KNO scaling of $p + A \rightarrow h^{\pm} + \cdots$ corrected for the positive excess for various targets at different energies. Note that scaling holds only in the forward direction corresponding to the fragmentation of the proton projectile.

Fig. 13. Comparison of the measured charged multiplicity of p + A with the predictions by the semi-empirical formula (17).

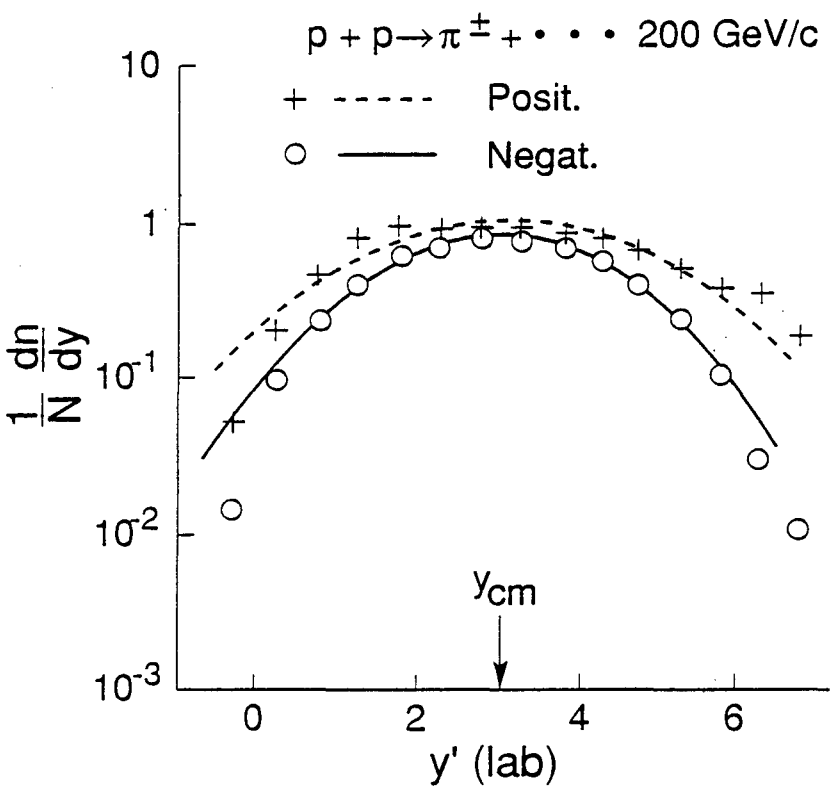

XBL 908-5549

Fig. 1

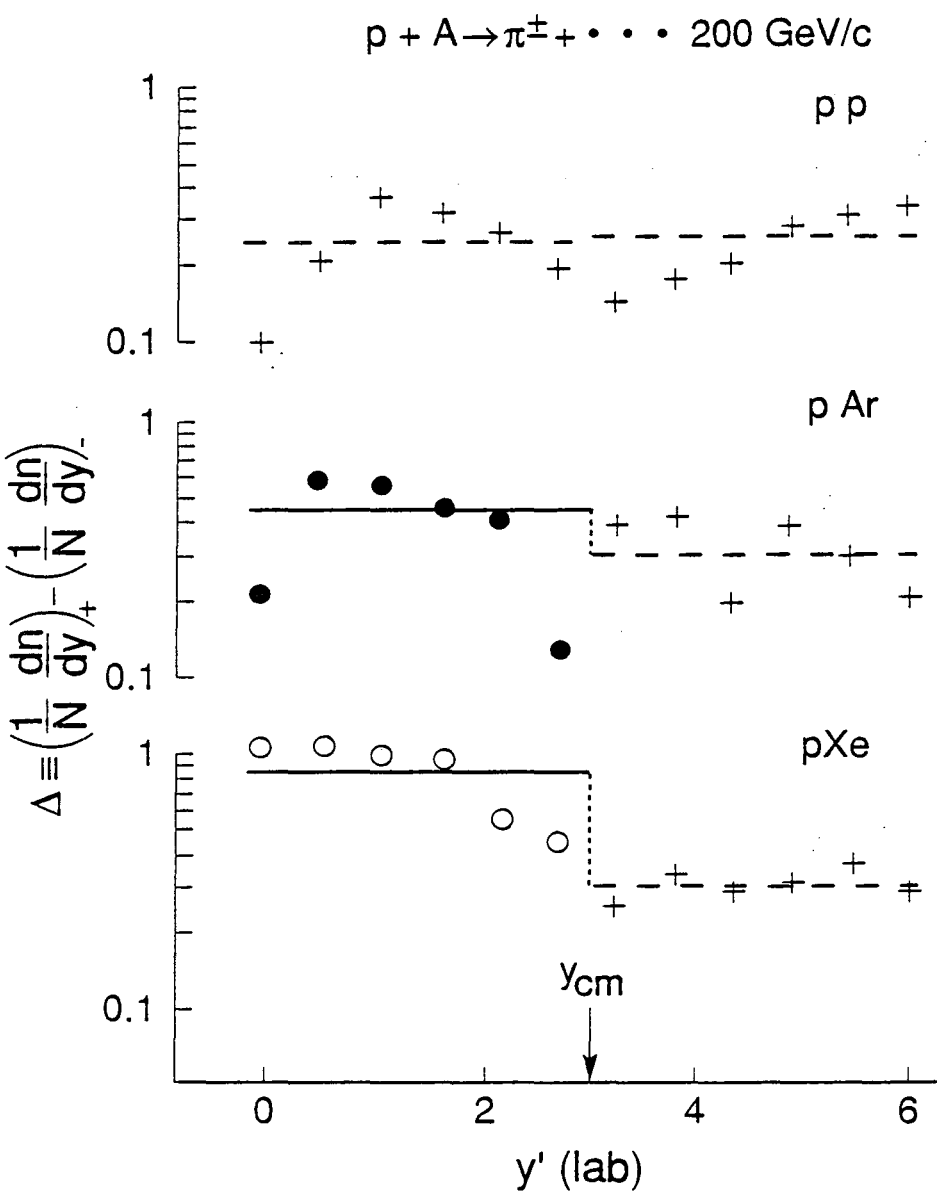

XBL 908-5550

Fig. 2

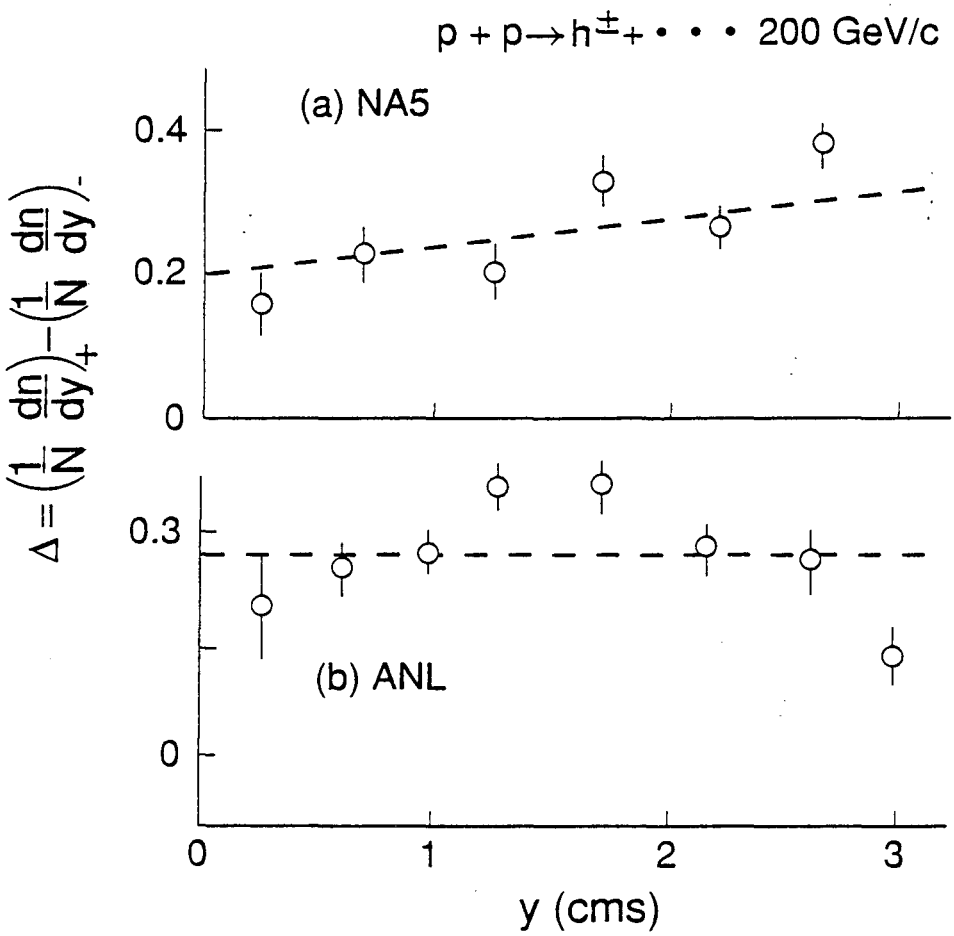

XBL 908-5551

Fig. 3

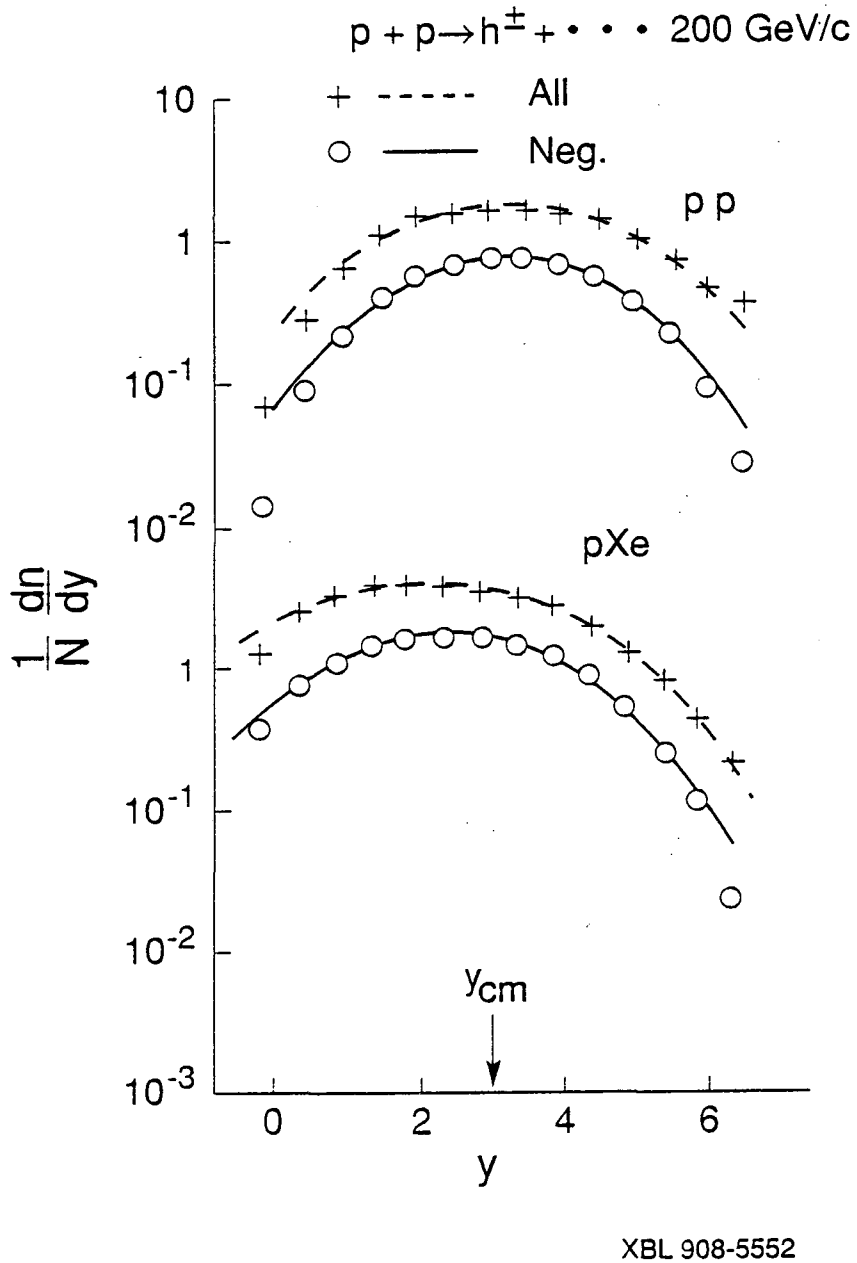
p + p→h± + • • • 200 GeV/c
All
Neg.
p p
pXe
1/N dn/dy
10
1
10-1
10-2
10-3
ycm
0
2
4
6
y
XBL 908-5552

Fig. 4

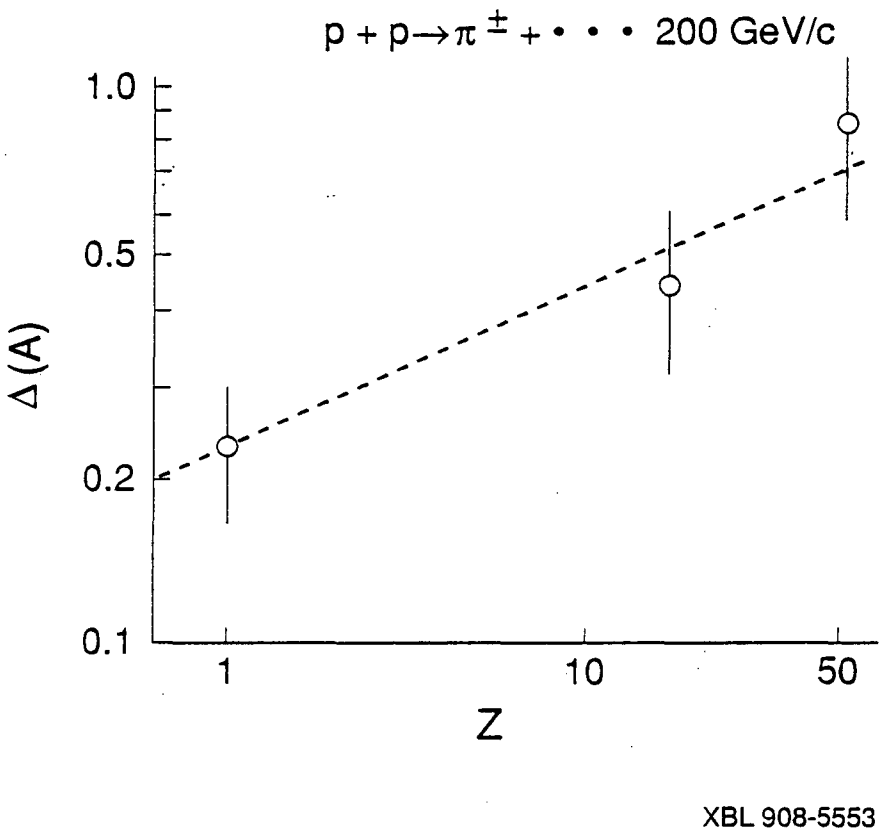

Fig. 5

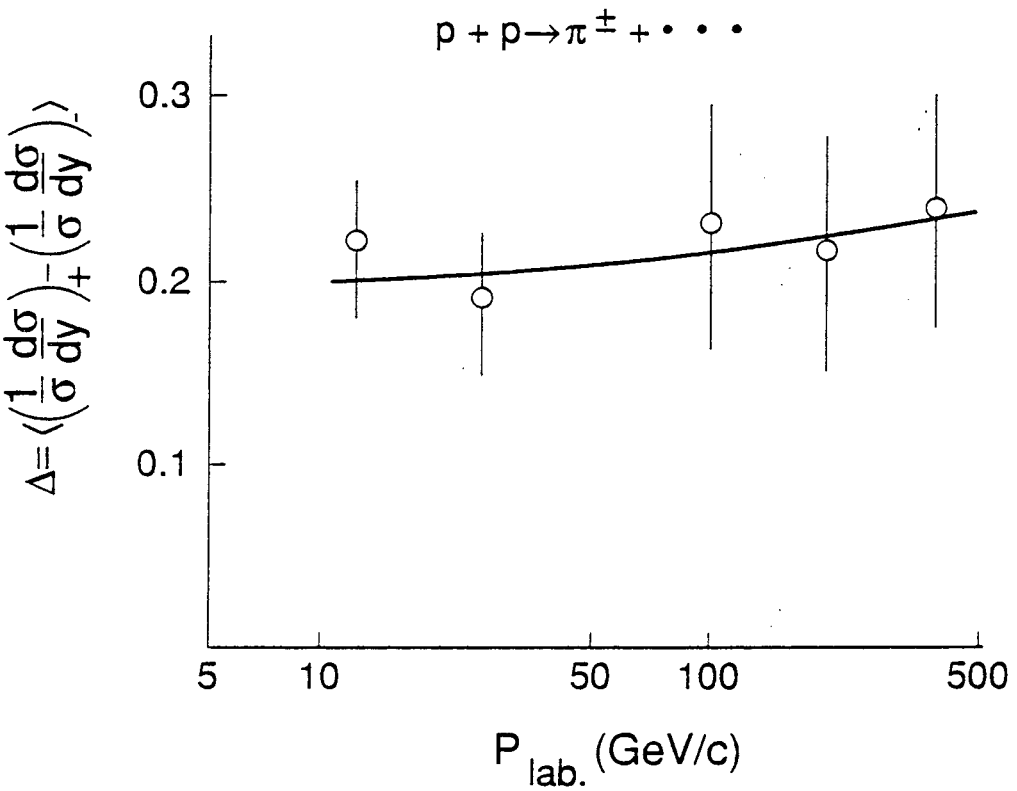

XBL 908-5554

Fig. 6

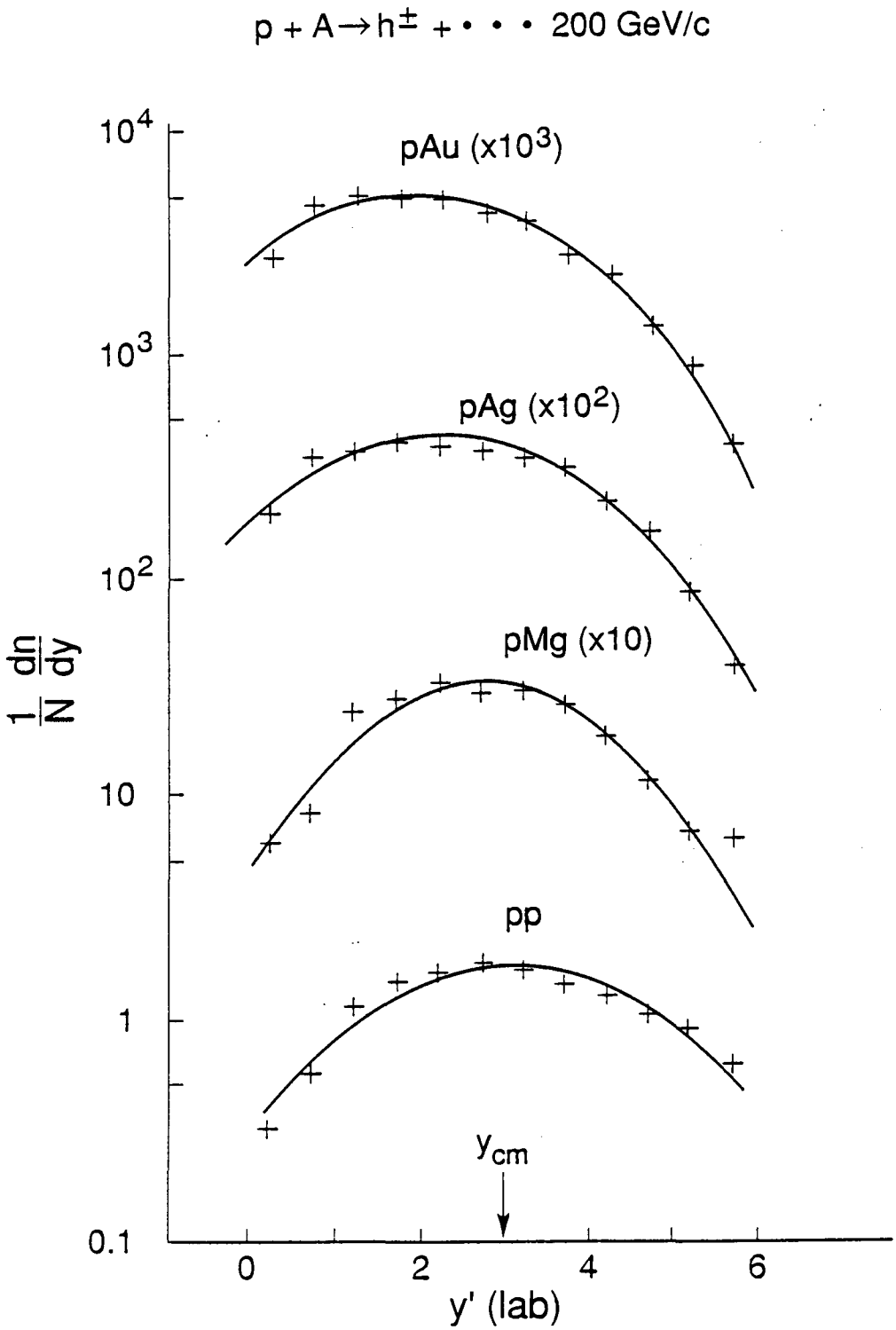

XBL 908-5555

Fig. 7

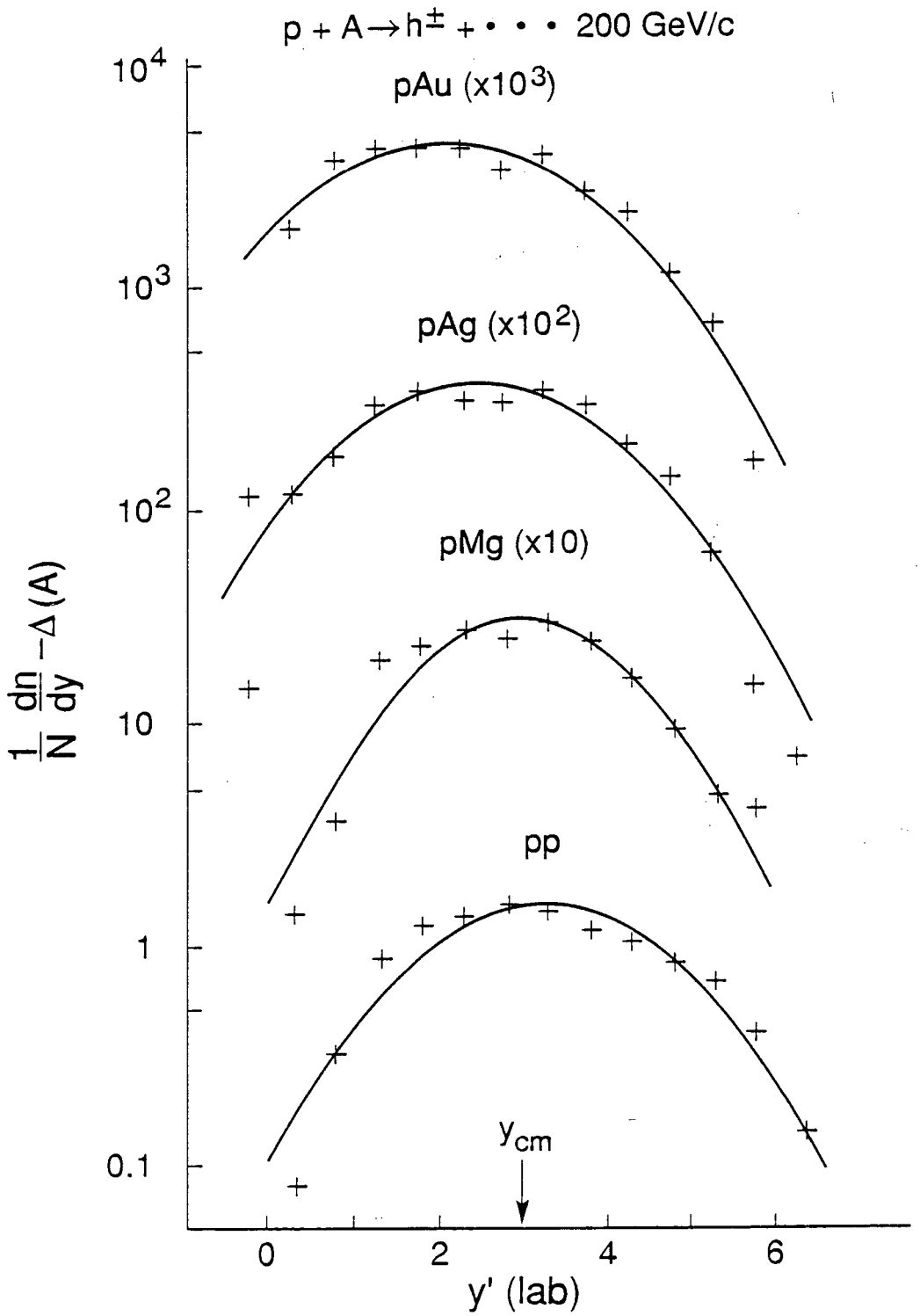

XBL 908-5556

Fig. 8

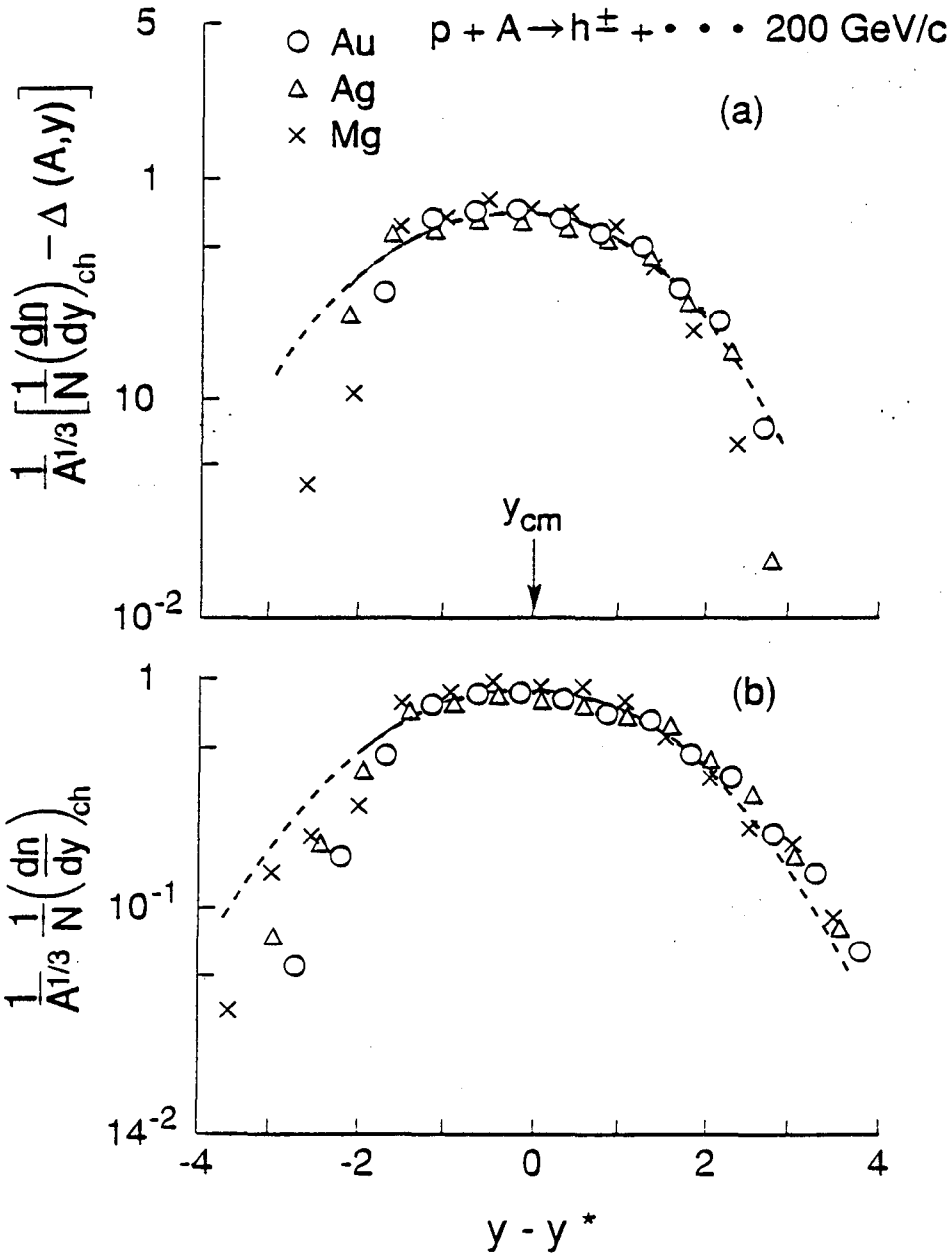

Fig. 9

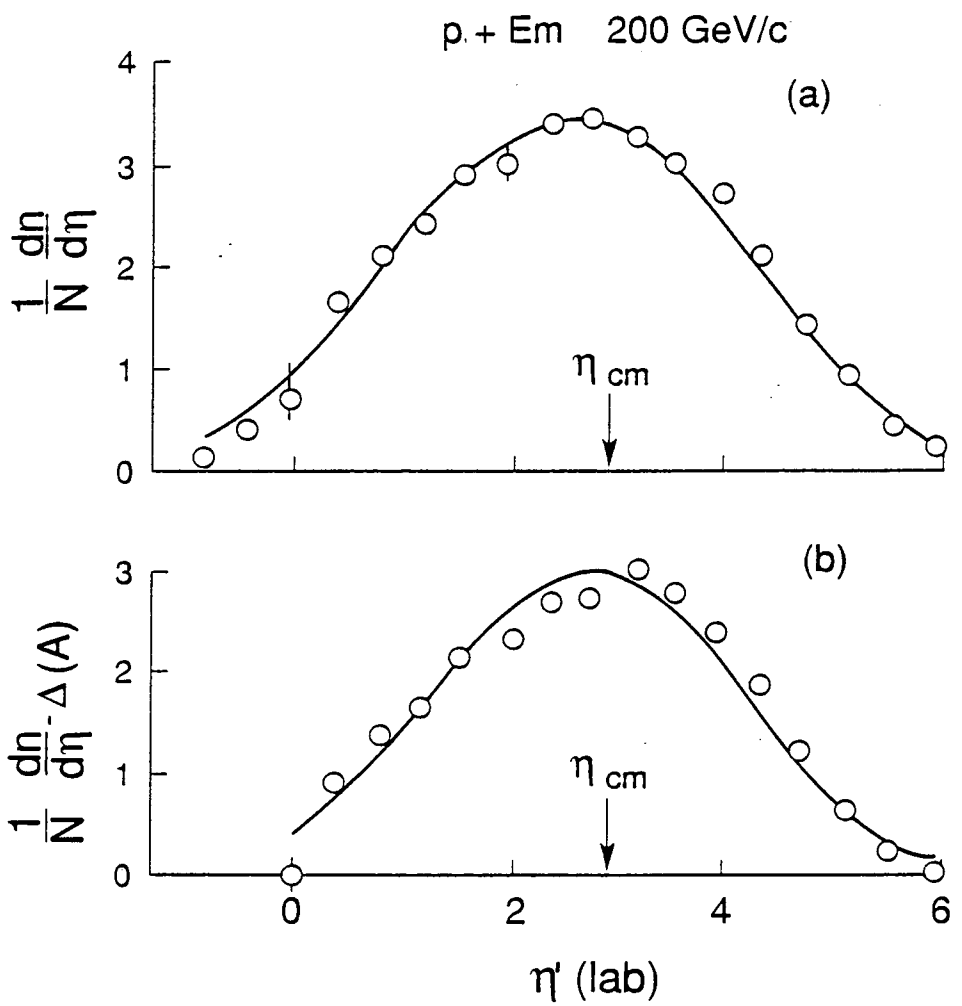

XBL 908-5558

Fig. 10

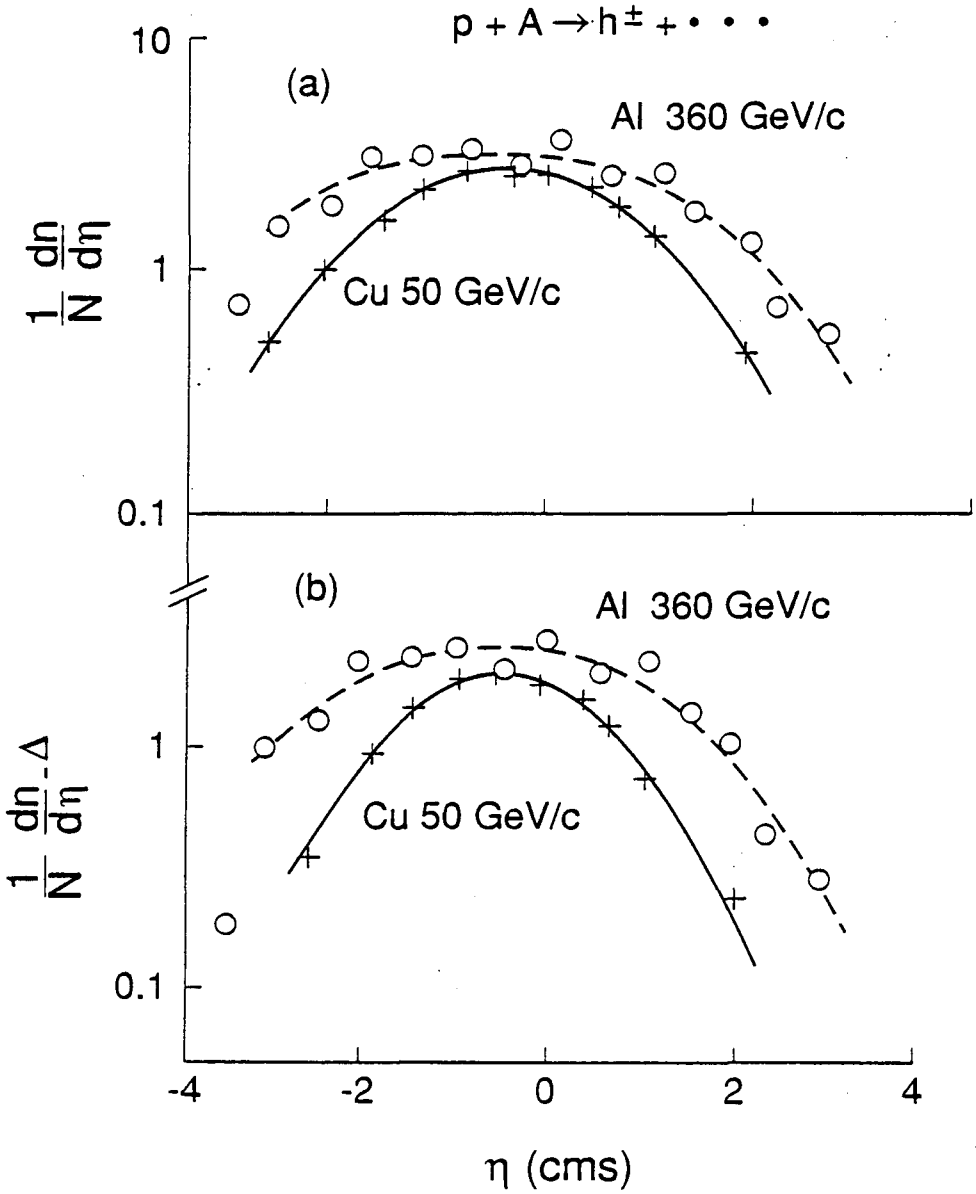

XBL 908-5559

Fig. 11

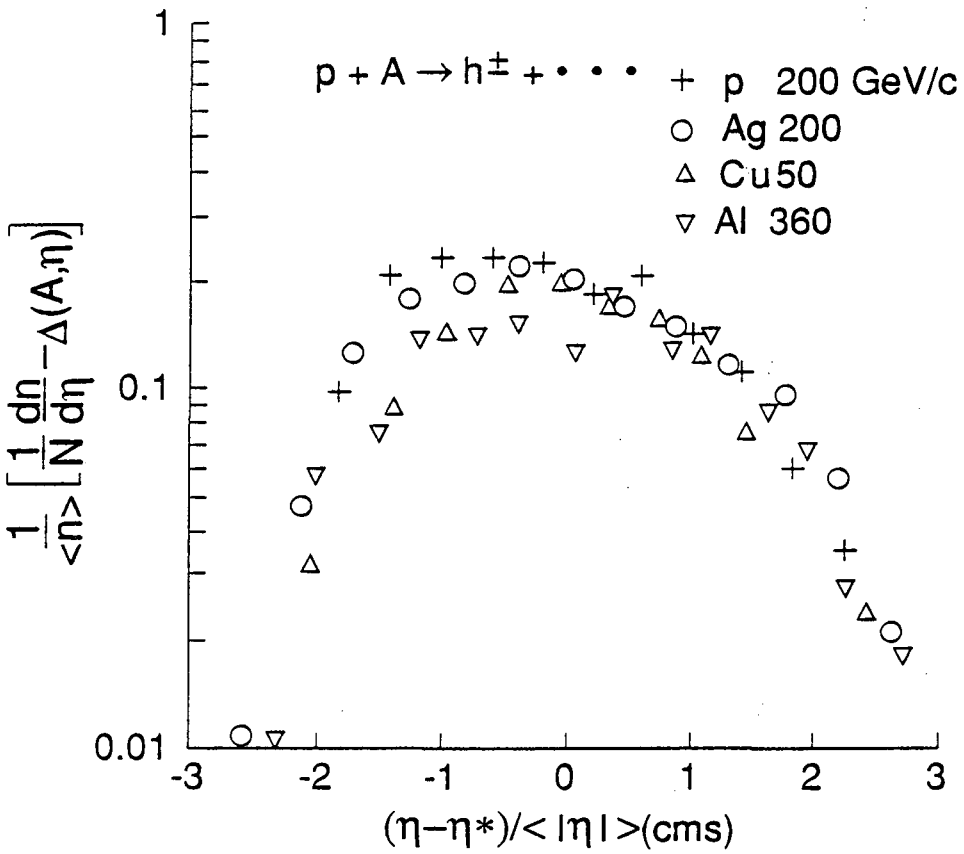

XBL 908-5560

Fig. 12

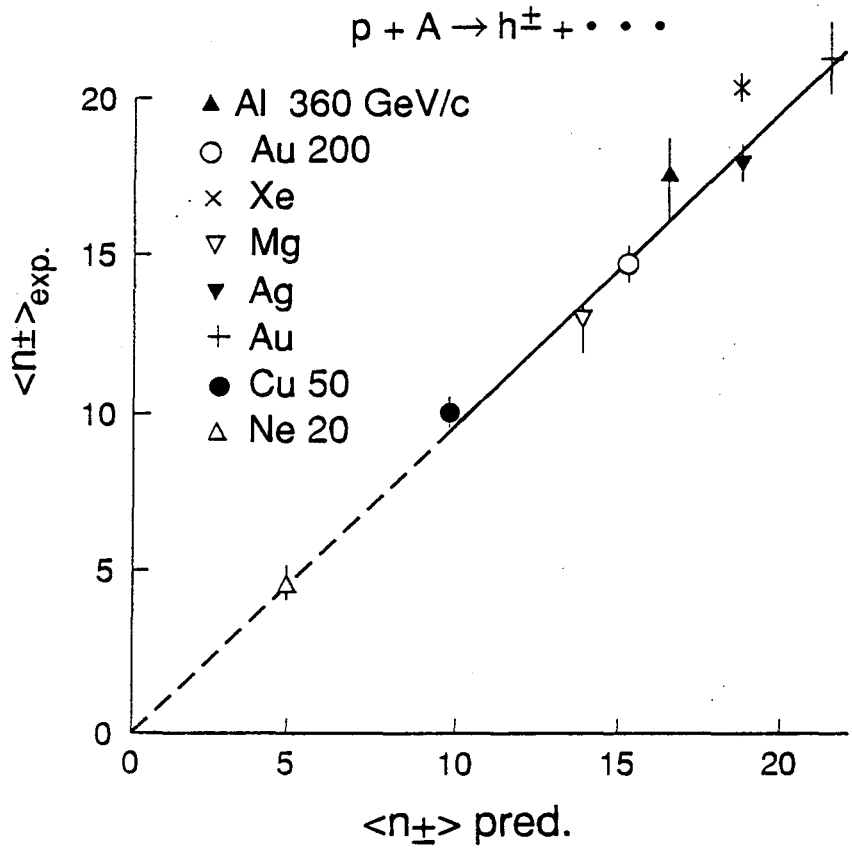

XBL 908-5561

Fig. 13

LAWRENCE BERKELEY LABORATORY
UNIVERSITY OF CALIFORNIA
INFORMATION RESOURCES DEPARTMENT
BERKELEY, CALIFORNIA 94720